PERFORMANCE ANALYSIS OF UNMANNED AIR VEHICLE INTERCEPTOR (UAV-Ip)

FLT LT MUHAMMAD ASIM
AHQ CHAKLALA (PROJ VISION) RAWALPINDI
PAKISTAN AIR FORCE, PAKISTAN
a007pk@ yahoo.com and aero49er@ yahoo.co.in

Key word: UAV-Ip

Abstract

Use of the Unmanned Aerial Vehicle (UAV) has existed for many years for a variety of different tasks. In previous years, UAV missions have included reconnaissance, surveillance, bomb damage assessment (BDA), scientific research, and target practice. However, UAV's have never been widely used in direct combat. Even current high-tech UAV's such as the Darkstar are limited to non-combative missions. In an age when the physiological tolerances and physical capabilities of the crew restrain the limits of performance of a modern fighter, the use of a UAV in a combat role deserves some consideration. This paper elaborates the aerodynamic and performance analysis of UAV that can be used as interceptor and can perform reconnaissance/surveillance missions as well.

1 Design Philosophy and Goals

The principle goal in the UAV-Ip (Unmanned Aerial Vehicle - Interceptor) design process was to create an interceptor, which could super cruise to intercept a target in a minimal time at a maximum possible range. The application of this aircraft would be defensive in nature, when conventional aircraft are immediately unavailable or unable to deploy. The UAV-Ip would be preprogrammed to carry out a certain mission.

2 Design Requirements

A set of requirements was set for the UAV-Ip in order to accomplish mission effectively and efficiently. These requirements are:

- Payload - Four AMRAAMs weighing just under 1500 lbs.
- Dash - A 320 nm range in 20 minutes from launch.
- Range/Radius - 700nm with a 15 minute loiter/350nm radius.
- Avionics - Capability of launching all missiles given targeting information from friendly ground, sea or air based platforms. GPS/INS for accurate location of the UAV-Ip and for navigation and guidance. Yaw, pitch, roll, temperature, fuel & RPM sensors for flight control. Radio for data up & down link.
- GPS receiver for accurate location of aircraft.
- On Board Sensors - The mission sensors include video and IR cameras for day & night surveillance and reconnaissance
- Take-off/Landing - Capable of either a land or sea take-off and landing.
- Ground Control Station (GCS) – To control and monitor the UAV-Ip and display reconnaissance information.

2.1 Mission Profiles

2.1.1 Primary Mission: Intercept

The primary mission of the UAV-Ip is characterized by a high-speed dash to the target area, followed by an immediate payload release

and return to base. This mission is represented below in figure 2.1.1

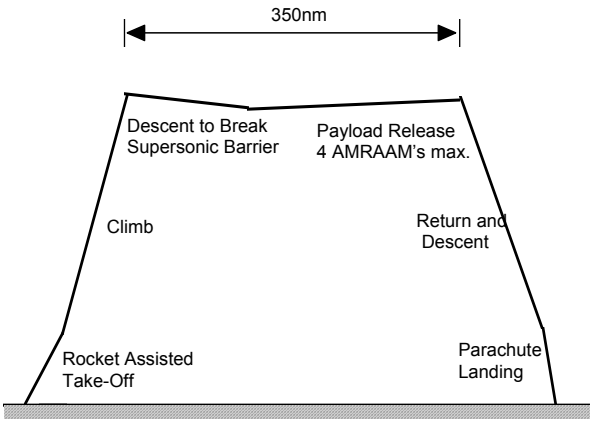

Figure 2.1.1 Primary Mission Profile: Intercept

2.1.2 Secondary Mission: Combat Air Patrol / Reconnaissance

In contrast, the secondary mission of the UAV-Ip is characterized by a fuel-efficient subsonic cruise to the target area. Figure 2.1.2 below shows the stages of the secondary mission

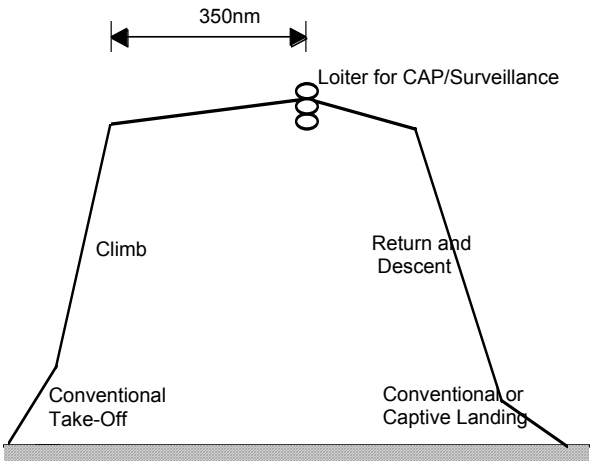

Figure 2.1.2 : Secondary Mission: Combat Air Patrol / reconnaissance

The mission proceeds with a conventional take off and climb to an optimum cruising altitude. The aircraft then enters a subsonic cruise stage in which fuel is conserved to a necessary degree, depending upon the mission. Upon reaching the target area, the UAV-Ip will have the capability to loiter within a specified combat radius for a maximum of 15 minutes.

At this point, there are numerous tasks that the UAV-Ip can be equipped for, including, but not limited to, the following: air combat, radar platform, surveillance, anti-ship, electronic warfare, etc. The likely role in this mission would be combat air patrol, in which the UAV-Ip would loiter in an area of suspected enemy air activity.

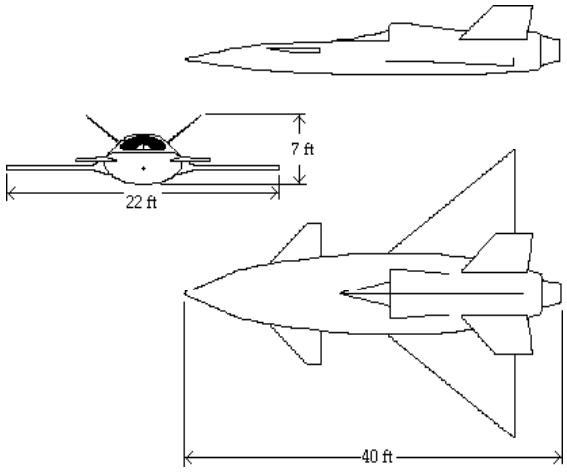

Figure 2.2: Three Views Drawing of UAV-Ip Conceptual Design

3.0 Aerodynamics

The aerodynamic characteristics of an aircraft are vital in obtaining the finalized aircraft configuration. Rough estimates of the aerodynamics, weights, and propulsion characteristics were utilized to find the initial sizing of the aircraft. Studying and calculating the aerodynamic forces acting on the aircraft, the initial design of the aircraft was analyzed

and iterations were performed to determine the best combination of design parameters. These design parameters then led to a resizing of the initial aircraft configuration in order to meet the given mission and performance speculations at the minimum weight and cost.

3.1 Airfoil Section

Many factors must be considered in the selection of the airfoil to be used for the wing, canards, and V-tail. Some of the concerns are with the aircraft capabilities, while others are with the aircraft configuration. The UAV-Ip is to perform a majority of its maneuvers in the supersonic region. Therefore, to be able to perform in the supersonic region the NACA 64-004 airfoil was chosen. It is a very thin, symmetric airfoil. It has a 4% thickness to chord ratio with the maximum thickness at 40% of the chord length. In addition, the symmetry allows for a lower C_d at higher C_l. The airfoils for the V-tail (NACA 64-005) and the canard (NACA 64-003) are also symmetric for simplicity and have a small thickness ratio for the same reasons as the wing. The canard has a smaller thickness to chord ratio than that of the wing to increase the critical Mach number so that shocks form first on the wing rather than on the canard.

3.2 Lift

The lift-curve of the aircraft depicts the relationship between the aircraft's lift coefficient and the angle of attack. The slope of the lift-curve is needed during conceptual design for three reasons. First, the lift-curve slope is used to set the wing incidence angle, which influences the required fuselage angle of attack during takeoff and landing and in turn the landing gear length and aft fuselage upsweep. Secondly, the methodology for calculating drag-due-to-lift for high performance aircraft requires a knowledge of the lift-curve slope. Thirdly, the lift-curve slope in conceptual design is for longitudinal-stability analysis.

3.2.1 Subsonic Lift-Curve Slope

Before the three-dimensional lift-curve of the aircraft could be obtained, it was necessary to determine the two-dimensional lift-curve of the airfoil. This was accomplished by an analysis of the wing airfoil through a program called PANDA developed by Desktop Aeronautics of Stand ford, California. PANDA, or Program for the Analysis and Design of Airfoils, was primarily utilized in confirming the two-dimensional flight parameters of an airfoil found by VMAX and illustrated in historical lift-curve charts. PANDA is capable of performing in viscid lift and drag calculations for a user inputted airfoil. The program allows for a determination of four of the two-dimensional airfoil's most useful parameters for a given Mach number: zero-lift angle of attack, maximum lift coefficient and corresponding angle of attack, or "stall" angle, and the slope of the airfoils lift-curve line. It is useful to note that the actual maximum lift coefficient and stall angle are not directly calculated by PANDA. The program does calculate the point on the airfoil were turbulent separation occurs. An analysis of turbulent separation with different angles of attack allows for a more accurate evaluation of the stall characteristics of the airfoil, including the stall angle and the maximum lift coefficient.

Once the two-dimensional lift parameters are obtained, equation (1) can be utilized to obtain the expected three-dimensional lift-curve slope (per radian) of the aircraft. The equation is accurate up to Mach 1.

$$C_{l\alpha} = \frac{2\Pi A}{2 + \sqrt{4 + \frac{A^2\beta^2}{\eta^2}\left(1 + \frac{\tan^2 \Lambda_{\max t}}{\beta^2}\right)}} \left[\frac{S_{\exp o}}{S_{ref}}\right](F) \qquad (1)$$

Where

$$\beta^2 = 1 - M^2 \qquad (2)$$

$$\eta = \frac{C_{l\alpha}}{2\Pi/\beta} \qquad (3)$$

In the above equations, $\Lambda_{max\,t}$ is the sweep of the wing at the maximum thickness location, and $S_{exposed}$ is the wing's exposed plan form area. The fuselage lift factor, F, accounts for the fact that the fuselage of a diameter, d, creates some lift due to the "spill-over" of the lift from the wing. The equivalent fuselage diameter is zero for the canard and the V-tail because it was assumed that lift for the fuselage of the aircraft was accounted for by the calculations performed on the wing.

3.2.2 Supersonic Lift-Curve Slope

The UAV-Ip is going to maneuver mostly in the supersonic region. The effect of the supersonic region on the aircraft is when the leading edge of the airfoil is located within the Mach cone.

where

$$C_{L\alpha} = 4/\beta \qquad (4)$$

$$\beta = \sqrt{M^2 - 1} \qquad (5)$$

when

$$M > 1/\cos\Lambda_{LE} \qquad (6)$$

As mentioned before, PANDA is only accurate up until Mach 1 for predicting the lift-slope curve. It is quite difficult to predict the lift-curve line with out utilizing hi-tech aerodynamic programs and computational fluid dynamics, but Raymer and other references provide alternate methods in calculating supersonic aerodynamic lift characteristics of a wing. Raymer utilizes the taper ratio, leading edge sweep, and wing aspect ratio to find the lift-curve slope of the UAV-Ip in the supersonic region. The charts in Raymer Fig. 12.6 represent data for wings of a different taper ratio and use the aforementioned values to estimate the slope of the normal force coefficient (Cn), the lift-curve slope in the direction perpendicular to the surface of the wing. For low angles of attack this value is approximately equal to the lift-curve slope.

3.2.3 Transonic Lift-Curve Slope

The lift-curve slope for the transonic region is found by utilizing both the subsonic and supersonic lift-curve lines. The transonic lift-curve line is estimated by plotting the supersonic and subsonic lift-curve lines simultaneously by iterating a smooth curve between the two.

3.2.4 Maximum Lift and Stall Angle (zero flaps)

The wing area of an aircraft is found by using the maximum lift coefficient of the wing. This influences the aircraft's take-off weight and cruise drag, but maximum lift estimation is not the optimum choice for initial aircraft conceptual design. Raymer does provide a method for estimating the lift coefficient and stall angle for aircraft traveling at low velocities (Mach 0.2). The first step is to determine whether the wing is classified as either a high- or low-aspect ratio wing through an algebraic test of the wing geometry. Once the wing aspect ratio has been classified as either high or low, a series of charts in Raymer allows the determination of the maximum lift coefficient and the maximum angle of attack of the wing.

3.2.5 Aerodynamic Results for the UAV-Ip

The methods described in section 3.2 were utilized to obtain the lift-curve, or lift coefficient vs. angle of attack, for the UAV-Ip conceptual design. The effect of Mach number on the lift-curve slope is illustrated in figure 3.2.1 The UAV-Ip data is compared to other 2-D airfoil line boundaries.

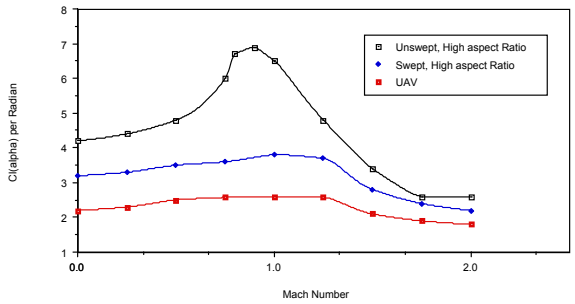

Figure 3.2.1: Lift-Curve Slope vs. Mach Number

The subsonic lift-curve was calculated utilizing a speed at a low Mach number (0.2). For this Mach number the lift-curve slope, as well as estimates of the maximum lift, stall angle, and zero lift angle of attack were obtained, see figure 3.2.2.

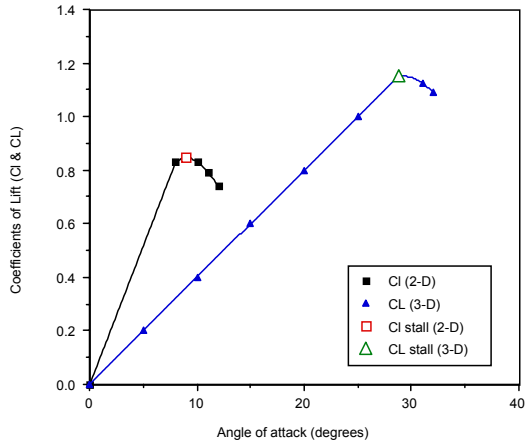

Figure 3.2.2: Clean Wing Lift Curve (Subsonic, Mach 0.2)

Figure 3.2.3 illustrates the supersonic, a Mach number of 1.8, lift-curve slope. The data is plotted against the subsonic lift-curve slope. The slope is very high; therefore, the aircraft must not perform high maneuvers at this speed. The estimates for the maximum lift coefficients and maximum angle of attack have not been obtained. For this reason, the supersonic lift-curve plotted is shown for a reasonable range of angles of attack only and should not be used to infer the maximum angle of attack or maximum lift coefficient for the aircraft.

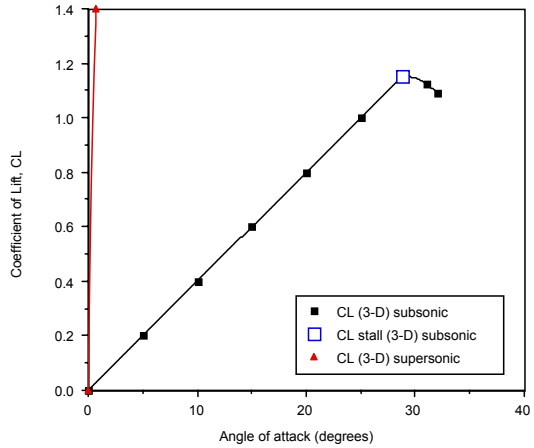

Figure 3.2.3: Clean Wing Lift Curve (Supersonic, Mach 1.8)

The lift-curve for the flapped aircraft was calculated and is illustrated in figure 3.2.4. The plot shows the effect of flaps on the aircraft for take-off and landing configurations.

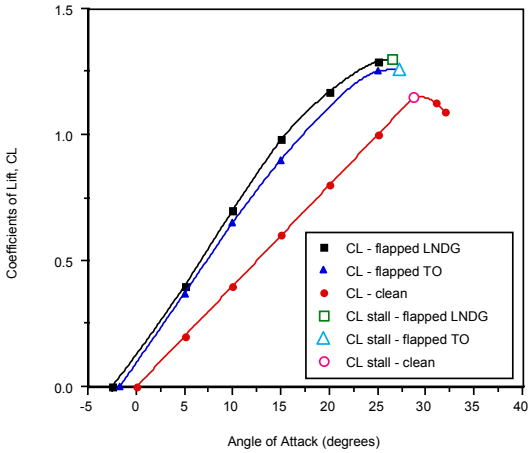

Figure 3.2.4: Flapped Wing Lift Curve (Subsonic, Mach 0.2)

3.3 Drag

Along with the benefits of lift comes the drawbacks of drag. An estimate of the drag on the airplane must be made to complete the aerodynamics and performance analysis. The first thing to consider is the parasitic drag, or the drag at zero-lift, which was calculated with a component buildup method. This method takes each component of the aircraft (i.e. wing, canard, V-tail, and fuselage) and calculates the skin friction drag coefficient (C_f), the form factor (FF) which estimates the pressure drag due to viscous separation, and an interference factor, Q, that estimates the interference effects due to the component. The total C_D for these components is calculated by using

$$C_{D_p} = \frac{\sum (C_{f_c} FF_c Q_c S_{wet_c})}{S_{ref}} \qquad (7)$$

where S_{ref} is the reference area of the wing.

In addition to these components, a C_D for the miscellaneous components of the aircraft is calculated (this includes flaps, unretracted landing gear, an unswept fuselage, etc.). The

final item to be considered is the drag from leakages and protuberances. An example of a leakage would be the gap between the wing and the flap, while examples of protuberances would be antennas and pitot probes. The total subsonic parasite drag was then calculated by summing all of the component coefficients of drag.

For supersonic parasitic drag, FF=Q=1.0 and the wave drag is included in the sum. Wave drag is the pressure drag due to shocks and is directly related to the area ruling of the aircraft. The wave drag is often greater than all the drags put together and therefore requires special attention when supersonic flight is required. The wave drag is calculated using empirical equations from Raymer. The estimate of the supersonic drag is based on historical data, due to the fact that this region is hard to predict and that the equations do not take in account the drag due to the formation of normal shocks in front of the inlet. The transonic parasite drag, which is the same basic equation as supersonic parasite drag, is estimated using industry defined equations. The values obtained allow for a rough estimate of the drag rise in the transonic regime due to the wave drag.

The overall parasite drag of the UAV-Ip is illustrated in figure 3.3.1 which plots the parasite drag versus the Mach number.

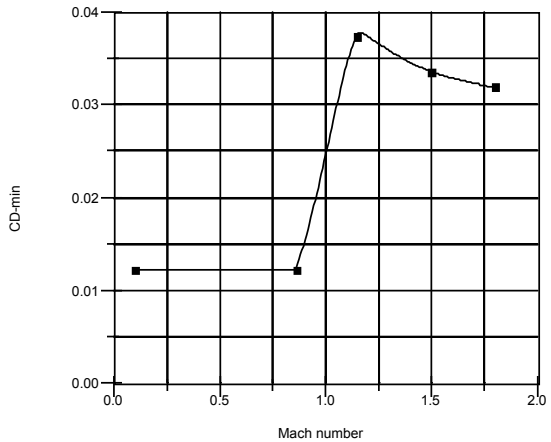

Figure 3.3.1: Overall Parasitic Drag of the UAV-Ip

The drag polar for the UAV-Ip was calculated by the use of VMAX. Since the wing is the primary lifting surface of the aircraft, this approximation will allow us to get rough estimate of the drag polar. The drag polar illustrated below in figure 6.3.4 is for both supersonic and subsonic cases. The drag polar equation for Mach .84 is $C_D=.0122 + .1980C_L^2$ and for Mach 1.8 is $C_D=.0319 + .4372C_L^2$

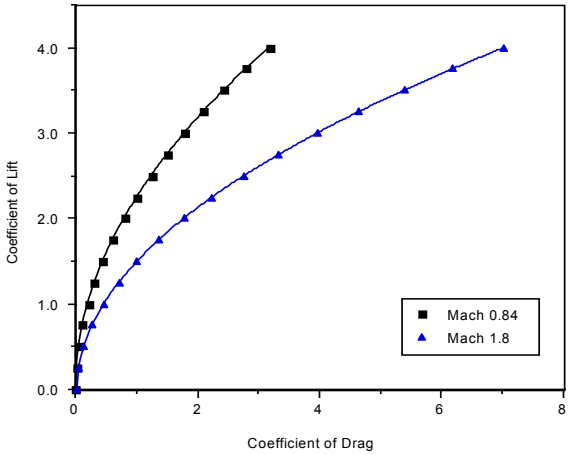

Figure 3.3.2: Drag Polar for the UAV-Ip

4.0 Performance

Performance is highly critical in design, particularly dash performance. The ability to super cruise at Mach 1.8 was deemed a necessity to meet requirements. Energy methods were used to determine the specific excess power which was used in calculations for the flight envelope, turn rate and climb. Other aspects considered in this section are loiter, cruise, takeoff and landing.

4.1 Energy Method

Specific excess energy (Ps) was used according to Raymer 17.87. Engine data is available for thrust as a function of Mach number and altitude. Cdo and K are available as functions of Mach number. Weight, though a function of time, was considered constant at 12,900 lbs (95% of takeoff weight), therefore, the results are at an average weight for the late climb and early cruise phases of the flight. This gave the most conservative energy for the cruise phase, yet still gave reliable results for the climb.Ps was first found as a function of Mach and altitude , which uses a load factor of one for steady, level flight.

The Ps is a measure of excess energy, thus wherever the Ps is positive or equal to zero, the plane can fly steady and level. So it can be seen that at sea level the maximum speed is about Mach 1.1. Maximum speed occurs at altitudes over 40,000 feet and is over Mach 2.1, though at this velocity, temperature limits should be considered to more fully define the flight envelope.

4.2 Flight Envelope

The flight envelope shows where the plane can fly in steady level flight. As mentioned before, if the energy is positive, then the plane can accelerate or climb. Conversely, if the Ps is negative the aircraft would be unable to maintain its velocity and altitude. Finally, the point at which Ps is zero, shows the normal limits on the aircraft, otherwise called the flight envelope.

Other limits were also used to constrain the flight envelope including maximum dynamic pressure (q), material temperature limits, and stall limits. A maximum dynamic pressure of 1800 psf (a conservative number for fighter aircraft, Raymer, p. 481) provided another constraint curve (Raymer, 17.95).

Temperature limitations (Raymer, 14.20) considered aluminum at the temperature limit of 250 F (Raymer Table 14.3). This limit was used to constrain the flight envelope, though actual points of high temperature on the aircraft body would use higher temperature materials such as steel or titanium.

Stall limited the low speeds, which as opposed to the Ps limit, considered a weight of 13,500 lbs to accurately reflect takeoff condition. The flight envelope is presented in figure 4.2.1, with all the above constraints.

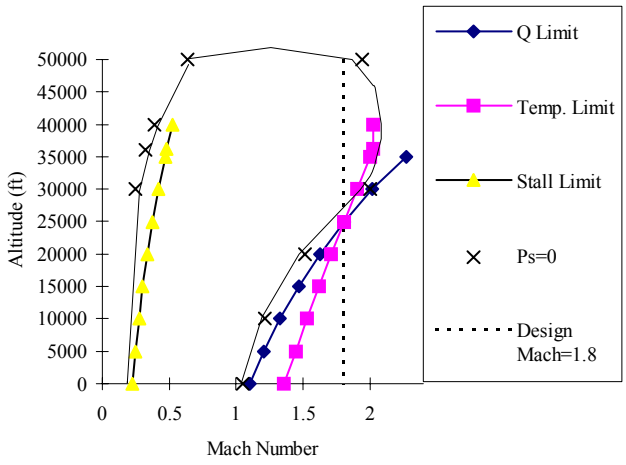

Figure 4.2.1: Flight Envelope

The shaded region of figure 4.2.1 is the flight envelope. The design point of Mach 1.8 at 35,000 feet is attainable and in fact the maximum Mach number is 2. The design point was determined to be the speed needed to meet our range and time requirements, while maintaining the lowest fuel consumption. From the flight envelope, it can be seen that the maximum altitude is at 50,000 feet, though it is not a constraint for this design. Further, as weight is decreased the maximum altitude will increase.

The low speed limit is obviously the stall limit which is about Mach .25 at sea level, up to a Mach of .4 at altitude. However, it is not expected that the UAV-Ip will fly near this point except for takeoff and landing, as our loiter velocity is substantially higher.

The high speed limit is limited by temperature to Mach 2.0. The temperature limit could be alleviated by use of higher temperature materials, as the calculations were performed for aluminum, and indeed the use of higher temperature materials is necessary to maintain stress and temperature limits. The temperature limit was left in place to show that temperature is indeed a major consideration near the design point.

Finally of note is the q limit, which is never reach in steady level flight, as the other

constraints are more restrictive. In a dive the q limit could be broken, particularly in the region of Mach 1.8 and 25,000 feet . In order to prevent this, the autopilot should be programmed to avoid breaking the q limit.

In summary, the flight envelope shows that the UAV-Ip can achieve the design goals of reaching a Mach of 1.8 at 35,000 feet. For off design points, there is a wide range of Mach numbers and altitudes under the design point, though going faster than the design cruise velocity may not be feasible as mentioned before due to temperature considerations. Fuel consumption for a Mach 2 cruise is actually less than the Mach 1.8 cruise, mainly from the decrease in time of flight to meet the dash range requirement. However, all performance calculations are based on a cruise Mach of 1.8, as a conservative figure since the plane was initially designed up to Mach of 1.8 and temperature and engine limits are being reached soon after Mach 2.0.

4.3 Climb

The climb profile is also defined by the Ps plot. For the intercept mission, time to climb is critical, which lends itself easily to energy methods. A plot of constant Ps curves as a function of altitude and Mach has been created and shown in figure 4.3.1.

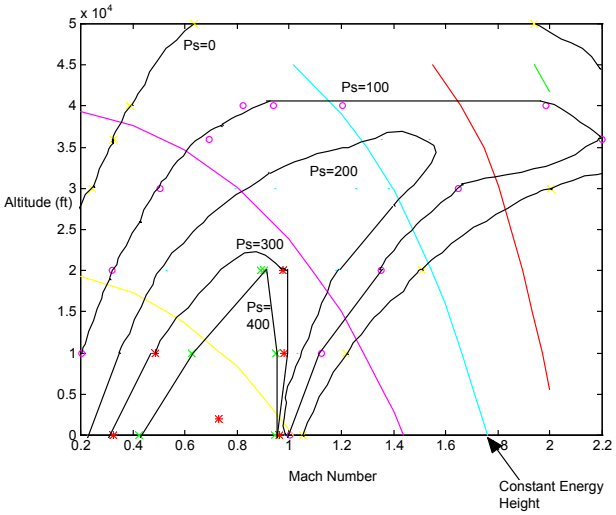

Figure 4.3.1: Altitude vs Constant Ps and Mach

By following a path of points defined by the tangent of the constant energy height curves to the constant Ps curves, the flight profile for the minimum time-to-climb trajectory is obtained. This profile is shown on figure 4.3.2.

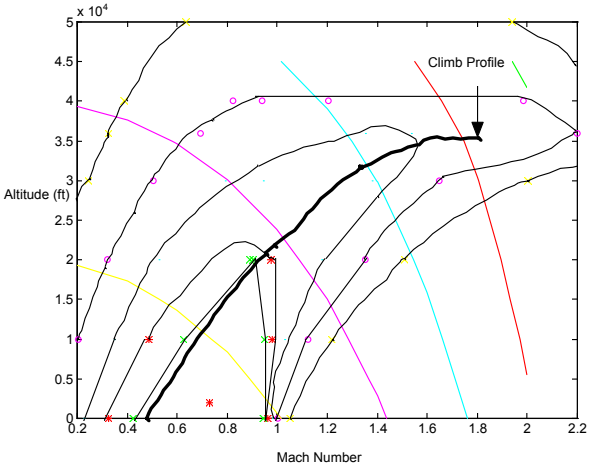

Figure 4.3.2: Minimum Time-to-Climb Trajectory, Energy Method

The time to climb can be found to be about 3.5 minutes (Raymer 17.90). From figure 4.3.3, the average velocity can roughly be determined for an average Mach number. This yielded an average horizontal distance of 50 nm. The fuel burned was calculated in a rough manner by taking an average velocity and altitude over the time to climb, which yields 580 pounds. This is an inexact calculation, so the time of climb (for this calculation) was assumed to be four minutes, instead of 3.5 minutes to be conservative.

4.4 Cruise

Cruise performance calculations were made for a Mach of 1.8 at 35,000 feet. This was the design point decided upon early in the design phase. In actuality, the aircraft can go faster as shown in the flight envelope, and actually burns less fuel. This comes from the fact that the UAV-Ip is slightly over-engined.

Important facets of the cruise are the time in flight to reach the design distance of

320nm, which must be less than the 20 minute requirement. Also, fuel burned is of critical importance as this portion of the mission burns the largest amounts of fuel. Time of flight was simply calculated as the time it takes to go 270 nm. The climb portion of the mission uses approximately 50 nm and 3.5 minutes, which leaves 270nm and 16.5 minutes. At he cruise condition, it takes 15.6 minutes to travel the remaining 270 nm.

Fuel is calculated based on the thrust for steady, level flight. Drag at this altitude and speed is approximately 6700 lbs, so thrust is approximately equal to the drag for small flight path angles. The TSFC can be determined knowing the altitude and thrust necessary from the partial throttle setting charts for 35,000 feet. Fuel burned is the product of the TSFC times the thrust (6700 lbs) and the time (.26 hrs). Total loss of fuel during the cruise is 1983 lbs, but this number was considered to be a little conservative, since the weight was only considered at one midpoint value for the cruise. Performance should increase as weight decreases, however, the induced drag term is small compared to the parasitic/wave drag term, such that the drag does not change significantly with weight, but mainly with speed and altitude.

4.5 Loiter

Project guidelines defined a 15 minute loiter after the cruise. Endurance can usually be defined for a jet as flying at the maximum L/D, that is the minimum thrust and maximum L/D (Raymer, eqns 17.13, 17.14, and pp. 458-459). However, this project's loiter calculations were not based on these equations, since the engine would need to be significantly throttled back, resulting in a possible dramatic rise in the TSFC. Iterations were made for Mach numbers of .4, .6 and .8, to find the drag and resulting thrust, tsfc and fuel consumed. Table 4.5.1 below shows the results for a weight of 12,000 lbs (a slightly conservative weight for post-dash).

Table 4.5.1: Loiter Fuel Estimations

Mach	Drag or Thrust	TSFC (lbs/hr)	Fuel lbs (1/4 hr)
.4	1395	.855	298
.6	967	.978	**236.5**
.8	1100	1.014	278.74

From this analysis, the minimum fuel burned was 236.5 lbs at Mach .6 at 35,000 feet.

4.6 Turn Rate

Turn rate was not required to be any particular value for the requirements, but should be reasonable. For a given altitude of 30,000 feet the maximum load factor can be found (Raymer, 17.52), which is used to determine the maximum sustained turn rate (Raymer, 17.50). Figure 4.6.1 shows the turn rate as a function of velocity.

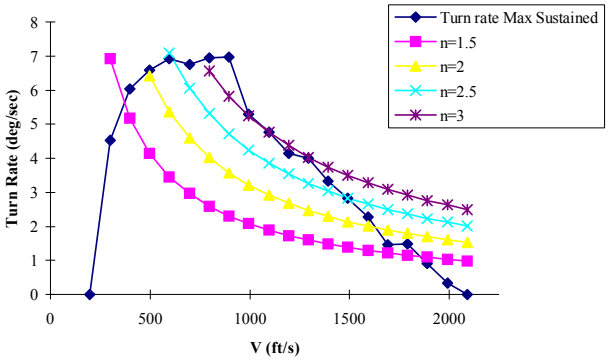

Figure 4.6.1: Turn Rate @ 30,000 feet

4.7 Return Cruise

The return cruise portion of the flight is a bit more ambiguous. The return weight of the aircraft is highly dependent on the fuel burned and how many missiles are shot. Also, the aircraft may be decelerating from Mach 1.8 to the cruise speed of Mach .8, or alternatively accelerating from the loiter speed of Mach .6. Raymer (p. 457) suggests a method for finding the velocity for best range, which unfortunately is a function of both the altitude and velocity. Using a set of solutions for velocity from Raymer (eqn. 17.25) and then calculating the drag, TSFC and time to return 250nm, the

optimum solution was found to be Mach .8 at 35,000 feet, with a fuel burned of 575 lbs over 39 minutes.

The above solution assumed a weight equal to burning all the fuel for a normal mission, but releasing none of the payload. This solution also assumes a constant return velocity, altitude and weight, but this is considered a conservative approach.

4.8 Descent

No fuel or flight path calculations were performed for descent. However this is a relatively short time and distance, so the fuel burned was 10% of the return cruise, or 57.5 lbs.

4.9 Takeoff and Landing

Takeoff and landing performance was concerned mainly with the ground roll distance. There is no requirement for takeoff or landing distance, however to increase the usefulness of the aircraft, these should be as short as possible. The maximum lift coefficient of 1.2 was used to find the takeoff speed, which is multiplied by a safety factor of 1.3. The calculated takeoff speed is 275 ft/s at sea level. Raymer's equation 17.99 was used to calculate the takeoff distance using the maximum takeoff weight, maximum sea level thrust, and an average coefficient of friction on dry concrete (Raymer Table 17.1). The resultant takeoff distance is 1365 feet.

A similar analysis was used for the landing distance, this time using the minimal thrust available at sea level, though keeping the landing speed the same at 275 ft/s and a modest weight loss of 500 lbs. A modest weight loss was used analyze an abort type landing. Using an average breaking coefficient, and the above numbers, equation 17.99 was again applied to yield 3265 feet of ground roll, including a 1 second period without breaks.

For a more typical landing, the ground roll is 2800 feet. This case assumed a much lighter airplane, thus a much lower landing speed. If these landing numbers are too long, it would be possible to increase the breaking, deploy spoilers or decrease the ground roll time by improved programming of the auto-pilot.

References

[1] Raymer, Daniel P., *Aircraft Design: A Conceptual Approach*, American Institute of Aeronautics and Astronautics, 1992.
[2] Whitford, Ray, *Design for Air Combat*, Jane's Publishing Inc., 1989.
[3] Munson, Kenneth, *World Unmanned Aircraft*, Jane's Publishing Inc., 1988.
[4] Nicolai, Leland M., *Fundamentals of Aircraft Design*, Self Published, 1975.